STATUS OF HIGH-POWER TESTS OF DUAL MODE SLED-II SYSTEM FOR AN X-BAND LINEAR COLLIDER*

Sami G. Tantawi, Christopher D. Nantista, Valery A. Dolgashev, SLAC, Menlo Park, CA94025

Abstract

Future linear colliders and accelerators require rf systems and components that are capable of handling multi-hundred-megawatt peak power levels at X band frequencies and higher. We present a set of RF components capble of handling these levels of powers. We also present a system implementation that uses these components. We carry out all of the RF manipulations in more easily handled over-moded rectangular waveguide. We present a smooth transition from circuilar to rectangular waveguide. This transition is perfected for two modes simultaneously. We show a set of rectangular overmoded components that can handle the same two modes simultaneously. Using these sets of components we constructed a fully dual moded rf pulse compression system. The system has produced 400 ns flat-top rf pulses of greater than 500 MW at 11.424 GHz. The system ran for hundreds of hours. After 39 million pulses the system tripped only 14 times; indicating the high reliability of these sets of components.

INTRODUCTION

Recently, ultra-high-power rf systems at X-band and above have received a lot of attention in different laboratories around the world because of the desire to design and construct a future linear collier. For a review of these activities the reader is referred to [1-2]. These systems are required to generate and manipulate hundreds of megawatts. Standard rf components that have been in use for a long time such as waveguide bends, directional couplers and hybrids, cannot be used directly because of peak field considerations. Usually, these components are made with oxygen-free high-conductivity copper and the operation takes place under ultra-high vacuum conditions. Experimental work at X-band showed that peak electric fields should not exceed 500 kV/cm [3]. Peak magnetic field should be limited so that the pulsed surface heating does not exceed 30 C^o [4].

To reduce the losses and to enhance the power handling capabilities one must use overmoded waveguides. Manipulating rf signals in highly overmoded waveguide is not trivial. With even simple functions, such as bends, the designs are quite complicated in order to insure the propagation of a single mode without losses due to mode conversion to other modes.

Also, most proposed designs for future linear colliders contain long runs of waveguides. In X-band room temperature designs, these runs are on the order of 100 km or more. To reduce the length of these waveguides, we suggested multimoded systems [5]. In these systems the waveguide is utilized multiple times, carrying different modes simultaneously. At first glance, one might think that this would lead to extra complications in the design of most rf components. Indeed, one has to invent a whole new set of multimoded components. However, since simple manipulations such as bending an overmoded waveguide tend to couple the modes together anyway, it turns out that designs of multimoded components are not much more complex. This is also true from the mechanical design point of view; most of these components are compact.

Manipulation of multiple modes in a single component can be easier in rectangular waveguide than circular. The philosophy of our designs is to do all the manipulation in two dimensions, i.e. planar designs. We leave the height of the waveguide as a free parameter to reduce the fields. To transport the the rf signals we need to use the low-loss circular waveguides. To take advantage of this, we present an rf taper which maps modes in circular waveguide into modes in rectangular guide. The modes of choice are TE$_{10}$ and TE$_{20}$ in rectangular waveguides and TE$_{11}$ and TE$_{01}$ in circular waveguides.

We present the design methodologies for these components, which can handle these two modes simultaneously. These designs feature smooth transitions to minimize field enhancements and at the same time they are virtually losses. We also present a pulse compression system based on these components. This system produced a peak rf signal of about 580 MW. In a reliability test, it ran for hundreds of hours at a power level of about 500 MW with pulse energy of more than 200 joules. The repetition rate varied from 30 Hz to 60 Hz. This exceeds the previous state of the art [3] by increasing the pulse energy by more than a factor of 3 and the pulse power by more than 25%.

DUAL-MODED CIRCULAR-TO-RECTANGULAR TAPERS

We assumed that all these tapers will be built using wire electron discharge machining (EDM). When tapering from one shape, e.g. a circle, to another shape, e.g. a rectangle, the length of the taper, *l,* and the connecting points between the two shapes uniquely define the taper. In cylindrical coordinates a shape *i* placed with cylindrical symmetry around the z-axis can be described by a relation $r_i(\phi)$, which gives the radius as a function of the angle ϕ. The taper between two shapes $r_1(\phi)$, and $r_2(\phi)$ is then given by $r(\phi,z) = r_1(\phi) + (r_2(\phi) - r_1(\phi))/l\ z$.

---

*This work is supported by the US Department of Energy, Contract number DE-AC03-76SF00515

Such a taper is compatible with the process of wire EDM when the two heads of the machine are moving synchronously with the same angular speed. More complicated tapers are constructed from a set of tapers, each of them have the above form, and then, cascaded together. First, let us consider an adiabatic taper between a square waveguide and a circular waveguide. We chose the dimensions of both the square and circular waveguides to be as close as possible, so that they both support approximately the same number of modes. The S-matrix of the transition connects modes of the same symmetry class, and for a sufficiently adiabatic transition preserves their TE (or TM) character.

The modes of interest in our application are TE$_{11}$ and TE$_{01}$ in the circular waveguide. These map to the TE$_{10}$ and both the TE$_{20}$ and TE$_{02}$ modes, respectively. Adiabaticity is sufficient to map the TE$_{11}$ in circular guide to the TE$_{10}$ in the square waveguide. However, one would want to convert the TE$_{01}$ mode in the circular guide to a single polarization of the TE$_{02}$ in the square guide. Modifying the square waveguide to a rectangular waveguide to break the degeneracy between the TE$_{02}$ and TE$_{20}$ modes could do this. However, in this case, the length of the taper required to achieve an adiabatic transition to a single mode in the rectangular guide is excessive. If one chooses the dimensions of the square waveguide and the circular waveguide such that the TE$_{02}$ circular mode and the TE$_{22}$ and TM$_{22}$ rectangular modes do not propagate, the length of this taper is approximately 18 cm at 11.424 GHz, or about 7 wavelengths. Instead, we construct this taper from three sections. The middle section is a cylinder with the with the shape: $r_2(\phi) = r_0(1 + 0.1\cos 2\phi)$, where r_0 is the radius of the circular guide.

The taper from the circle to the intermediate shape scatters the TE$_{01}$ mode into two modes M$_1$ and M$_2$ in the intermediate section. Also, the taper between the rectangular waveguide to the intermediate shape scatter the rectangular mode TE$_{02}$ into the same M$_1$ and M$_2$ modes. The lengths of both tapers are adjusted such that the coefficients of the scattered modes M$_1$ and M$_2$ are the same from both sides. Since M$_1$ and M$_2$ propagate with different phase velocities in the intermediate section, the length of that section could be adjusted so that the circular TE$_{01}$ mode gets completely converted into the rectangular TE$_{02}$ mode.

The idea of this design was first reported by our group in [6], later it was implemented to split the output of a TE$_{01}$ gyroklystron [7]. However, in both cases, no care was taken to insure the adiabatic propagation of the TE$_{11}$ mode. Because of the odd shape in the middle of this taper, described by Eq (2). The taper tended to couple the rectangular TE$_{01}$ to the circular TE$_{31}$ mode. This is not surprising, since that shape essentially contains a second-order azimuthal deformation which couples modes that differ in azmithal index by 2. On the other hand, the circular TE$_{11}$ mode is also coupled to TE$_{12}$ in the rectangular guide.

The design of was the result of several iterations on the design, increasing the length until a perfect conversion between one polarization of the TE$_{11}$ circular mode and the TE$_{01}$ (not TE$_{10}$) rectangular mode was achieved. Each time the length was increased, the full design was repeated to insure perfect conversion between the TE$_{02}$ rectangular mode and the TE$_{01}$ circular mode. Then the TE$_{11}$ circular to TE$_{01}$ rectangular conversion was checked. Fig. 1 contains field plots for the simulated taper performance, showing the mode conversion for the two modes.

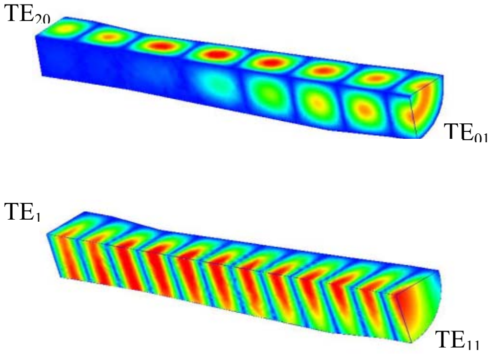

Figure 1: Simulated electric fields (HFSS) of the dual-moded circular-to-rectangular taper.

DUAL-MODED RECTANGULAR WAVEGUIDE SUPERHYBRID

The dual-moded rectangular super-hybrid, shown in Fig.2, is designed for our system using the overmoded rectangular waveguide planar design motif. The planar part of the device, is a four port device whose ports support the TE$_{10}$ and the TE$_{20}$ modes (actually TE$_{01}$ and TE$_{02}$ in this device, if one considers that the height is greater than the width). The cross-section tapers described above allow these ports to be connected to low-loss circular waveguide with one-to-one mode mapping. The planar design allows us to increase power-handling capability by building it overheight without having to take into account in our manipulations the additional propagating modes that this introduces, to which there should be no coupling.

The purpose of the super-hybrid is to pass the TE$_{20}$ mode from the input port through two ports to a resonant delay lines pulse compressor [3], combining identical reflections from these ports out the fourth port, while also allowing the rectangular TE$_{10}$ mode to be transmitted from input to output port by a different path, bypassing the pulse compressor. While the planar design allowed it to be machined out of a single block of copper, like a circuit on a substrate, it is actually composed of several subcomponents, designed individually.

The input port leads directly into a mode mixer, a slight jog or dogleg that couples the two modes. This converts a pure input of either TE_{10} or TE_{20} into an equal mixture of the two. This is followed by a dual-moded splitter, a T-junction, matched for both modes, which divides power from either pure mode equally between two single-moded (single moded in the horizontal plane only) ports. Proper spacing from the mode mixer allows the fields from each of the orthogonal mode combinations to cancel in one arm and add in the other. In combination, these two subcomponents serve to direct the power of the two possible input modes along different paths.

The input port leads directly into a mode mixer, a slight jog or dogleg that couples the two modes. This converts a pure input of either TE_{10} or TE_{20} into an equal mixture of the two. This is followed by a dual-moded splitter, a T-junction, matched for both modes, which divides power from either pure mode equally between two single-moded (single moded in the horizontal plane only) ports. Proper spacing from the mode mixer allows the fields from each of the orthogonal mode combinations to cancel in one arm and add in the other. In combination, these two subcomponents serve to direct the power of the two possible input modes along different paths.

A pair of mitred bends connects the power input as TE_{10} into an arm of a mirror image of the splitter. The mixed output at its overmoded port is then converted back to pure TE_{10} at the output port of the super-hybrid by a mirror image of the mode mixer. Perforation holes in the outer wall of the short waveguide section between mitred bends allows vacuum pumping in the heart of the device.

Power input as TE_{20} follows a similar path on the opposite side of the device. Here, the section between mitred bends is occupied by a planar hybrid of the Magic-H type [10]. Its coupled ports lead to mitred bends, which turn perpendicular to the power flow of the super-hybrid at a spacing designed to accommodate parallel highly-overmoded circular waveguide delay lines. Short width tapers, optimized with blended arcs, return to overmoded waveguide. These are followed by jog converters, which completely couple power between the two modes. The TE_{10} which came from the Magic-H ports, is thus converted to TE_{20} at the delay line ports of the device. This allows the rectangular to circular tapers to couple these ports to low-loss circular TE_{01} mode delay lines.

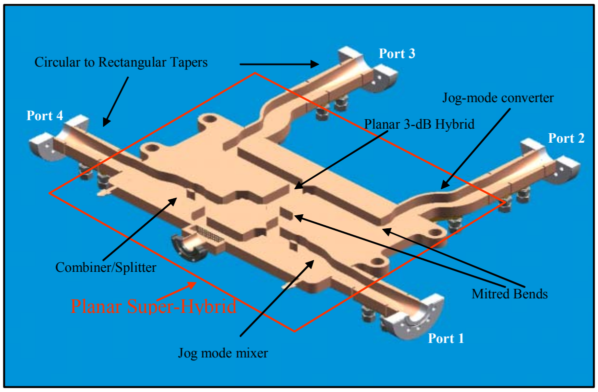

Figure 2: The design of the dual-moded superhybrid, a split view.

THE DUAL-MODED PULSE COMPRESSION SYSTEM

The Transfer Line Design

The components described above compose the heart of our dual-moded pulse compression system. The layout of our system is pictured in Fig. 3. WR90 waveguide carries the combined rf from each klystron pair to a port of a dual-mode combiner. This combiner is a three-port device, whose third port launches power from the single-moded inputs into overmoded circular waveguide in either the TE_{11} or TE_{01} mode, depending on the relative phase of the inputs.

The total combined power is fed into the super-hybrid described above. With the klystron pairs phased to launch TE_{01} into the system, power is directed through the resonant delay line [3,12,13]. These lines are also dual-moded. In the following subsection we give a brief description of this dual-moded pulse compressor. However, for a detailed design of the dual-moded delay lines, the reader is referred to reference [13].

By the opposite phasing, power is directed around an alternate path to the same dual-mode output port. Thus, the system can be run in compressed (TE_{01}) or uncompressed (TE_{11}) mode. Before and after the superhybrid are dual-mode directional couplers in circular waveguide for monitoring the power in each operating mode. The design of this coupler essentially follows the procedure outlined in [14].

A splitter similar to the combiner divides the output power from either operating mode between two arms, each of which further divides the power again in four, so that it can be sent into eight high-power loads.

The Pulse Compressor Delay Lines[13]

The pulse compressor consists of two highly-overmoded, iris-coupled, resonant delay lines, attached to two additional ports on a hybrid section of the super-hybrid. These delay lines, roughly 30 m long in 17 cm diameter circular waveguide, are also dual-moded. Here dual moding refers to the fact that they are designed to operate in both the circular TE_{01} mode and the circular TE_{02} mode, simultaneously. A mode converting reflector at the end of each line transfers power between these two modes. Since TE_{02} is cut off at the input taper of each line, it takes two round trips between each time the wave can impinge on the coupling iris. This effectively doubles the delay time for a line of given length, allowing the system to be considerably more compact than would be a standard delay lines for the desired compressed pulse width. The reflectors are mounted on accurately centered, stepping-motor driven vacuum feed-throughs for resonant tuning of the lines.

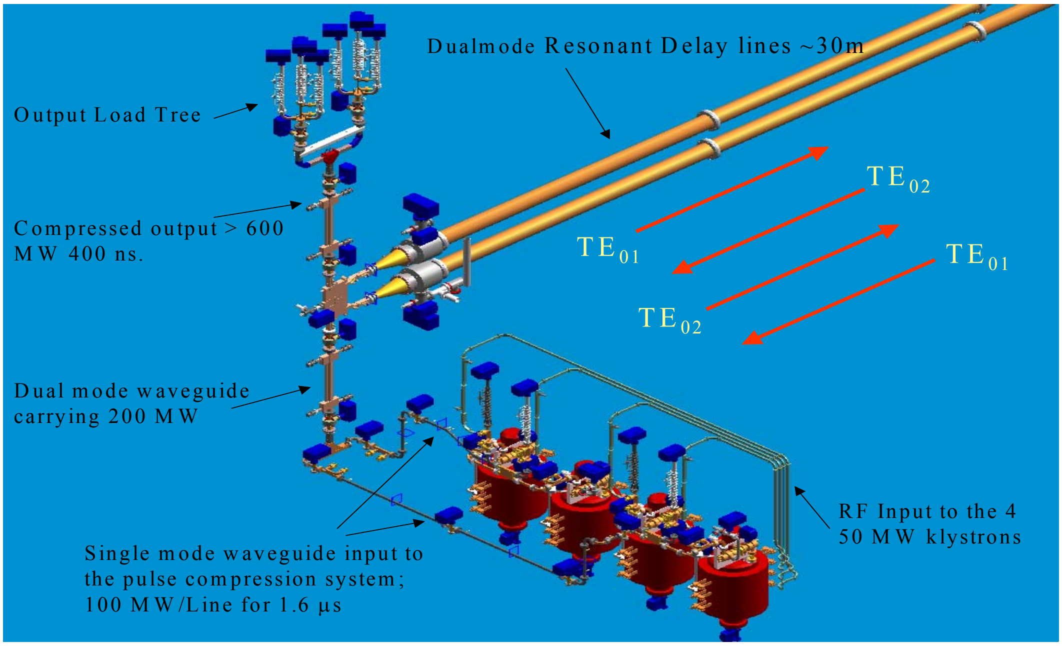

Figure 3: Isometric layout of the dual-moded RF system with dual-moded SLED-II pulse compressor.

TESTING AND OPERATION

Components were individually cold tested with a network analyzer. Results were quite satisfactory, with port matches and desired isolations typically somewhat better than -30 dB and losses on the order of a percent. The system itself was also cold tested at various stages of installation. Care was taken to avoid parasitic resonances, which can greatly degrade efficiency and can lead to dangerously high localized energy storage and field level

After completion of installation, the system was pumped down and carefully baked, after which vacuum levels on the order of 10^{-9} torr could be reached. Then high power operation commenced. While outgassing in the delay lines was a frequent cause of tripping our vacuum interlocks during processing, the main bottle neck was a faulty run of WR90 from the second pair of klystrons to the combiner.

Once this waveguide was replaced, processing progressed much more smoothly, and we soon reached our goal of more than 580 MW at full 400 ns pulse width. Further work on the the low-level rf drive system, incorporating arbitrary waveform generators and feedback optimization, allowed us to flatten the amplitude and phase of the pulse. Fig. 4 shows actual calibrated power meter measurements of the input and output pulses obtained.

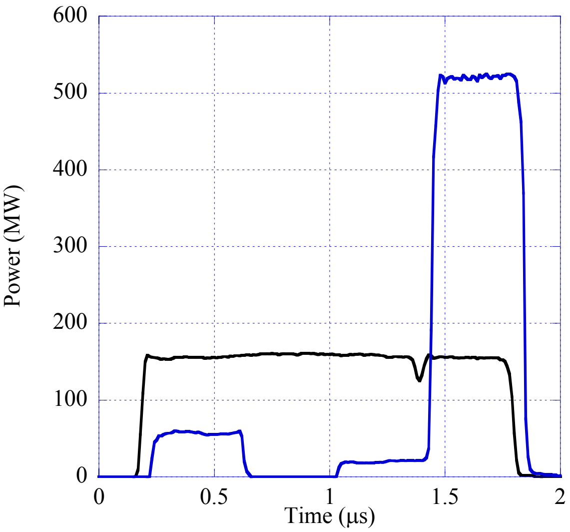

Figure 4: Power meter measurements of input (black) and output (blue) pulses during high power operation.

With this pulse shape and power level, slightly above 500 MW, we ran the system for more than 300 hours at a repetition rate that varied between 30Hz to 60 Hz. During this period the system produced more than 39 million pulses. The system tripped only 14 times; indicating the high reliability of these sets of components.

CONCLUSION

We presented the design of a set of components suitable for ultra-high-power operations at X-Band. This set of components comprises a dual-moded circular to rectangular taper and a set of planar dual-moded rectangular components. Using this set of components we constructed an ultra-high-power rf pulse compressor, which produced compressed pulses with power levels above 580 MW and ran regularly slightly above 500 MW. The pulse energy exceeded 200 joules. This achievement represents a milestone in demonstrating an X-band rf system suitable for the Next Linear Collider. It also represents the state of the art in generating coherent ultra-high-power rf signals.

ACKNOWLEDGEMENT

The authors wish to thank and acknowledge the contributions of all those who helped to attain this important goal, including physicists, engineers, operators, and technicians. We specially thank Jose Chan, Dennis Atkinson, David Schultz and the NLC group for their efforts during the mechanical engineering and construction of the project. We thank Richard Cassel and the modulator team for their continuous effort and support during the high power testing phase of this experiment, which was going on for 24 hours a day. We also acknowledge the efforts of Marc Ross, Janice Nelson, and the NLCTA operation group for their support during the testing phase of this project.

REFERENCES

[1] Physics And Technology Of The Next Linear Collider: A Report Submitted To Snowmass '96. By NLC ZDR Design Group and NLC Physics Working Group (S. Kuhlman et al.). SLAC-R-0485, BNL-52502, FERMILAB-PUB-96-112, LBL-PUB-5425, LBNL-PUB-5425, UCRL-ID-124160, Jun 1996. 197pp. See also BOOKS subfile under call-number: QCD191:S861:1996. Presented at 1996 DPF / DPB Summer Study on New Directions for High-Energy Physics (Snowmass 96), Snowmass, Colorado, 25 Jun - 12 Jul 1996.

[2] Sami G. Tantawi "New Development in rf Pulse Compression," LINAC2000-WE203, Aug 2000. 5pp., Invited Talk at the 20th International Linac Conference (Linac 2000), Monterey, California, 21-25 Aug 2000.

[3] Sami G. Tantawi, et. al. "The Generation Of 400-MW RF Pulses At X Band Using Resonant Delay Lines,", IEEE Trans. on Microwave Theory and Techniques, Vol 47, No. 12, December, 1999, p. 2539-2546

[4] V.A. Dolgashev, "High Magnetic Fields in Couplers of X-Band Accelerating Structures Proceedings of the 2003 Particle Accelerator Conference, Portland, Oregon U.S.A., May 12-16, 2003, pp 1267-1269.

[5] S.G. Tantawi, *et al.*, "A Multimoded RF Delay Line Distribution System for the Next Linear Collider," Phys.Rev.ST Accel.Beams, vol. 5, March 2002.

[6] Tantawi, S.G.; Kroll, N.M.; Fant, K.; "RF components using over-moded rectangular waveguides for the Next Linear Collider multi-moded delay line RF distribution system," Proceedings of the 1999 Particle Accelerator Conference, 1999. , Volume: 2 , 27 March-2 April 1999 Pages:1435 – 1437.

[7] Spassovsky, I.; Gouveia, E.S.; Tantawi, S.G.; Hogan, B.P.; Lawson, W.; Granatstein, V.L., " Design and cold testing of a compact TE_{01}^{o} to TE_{20} mode converter,", IEEE Transactions on Plasma Science, Volume: 30 , Issue: 3 , June 2002, Pages:787 – 793

[8] "HP High-Frequency Structure Simulator," HP EEsof, Hewalt Packard.

[9] AutoCAD, Copyright 1982-1998, Autodesk, Inc.

[10] Nantista, C.D.; Fowkes, W.R.; Kroll, N.M.; Tantawi, S.G.., "Planar Waveguide Hybrids for Very High Power RF," presented at the 1999 Particle Accelerator Conference, New York, NY, March 29—April 2, 1999; SLAC-PUB-8142.

[11] Sami G. Tantawi and A.E. Vlieks, "Compact X-Band High Power Load Using Magnetic Stainless," presented at the 1995 Particle Accelerator Conference, Dallas, TX, May 1-5, 1995; SLAC-PUB-6826.

[12] P.B. Wilson, Z.D. Farkas, and R.D. Ruth, "SLED-II: A New Method of RF Pulse Compression," presented at the Linear Accelerator Conf., Albuquerque, NM, September 10-14, 1990.

[13] S. G. Tantawi, "Multimoded reflective delay lines and their application to resonant delay line rf pulse compression systems," Phys. Rev. ST Accel. Beams 7, 032001 (2004)

[14] Tantawi, S.G.; "Mode selective directional coupler for NLC," Particle Accelerator Conference, 1993., Proceedings of the 1993 , 17-20 May 1993, Pages:1130 - 1132 vol.2.